



Novel 1D coordination polymer $\{\text{Tm}(\text{Piv})_3\}_n$: Synthesis, structure, magnetic properties and thermal behavior

Irina Fomina^{a,*}, Zhanna Dobrokhotova^a, Grygory Aleksandrov^a, Anna Emelina^b, Mikhail Bykov^b, Irina Malkerova^a, Artem Bogomyakov^c, Lada Puntus^d, Vladimir Novotortsev^a, Igor Eremenko^a

^a N.S. Kurnakov Institute of General and Inorganic Chemistry, Russian Academy of Sciences, Leninsky Pros. 31, 119991 Moscow, GSP-1, Russian Federation

^b Department of Chemistry, M.V. Lomonosov Moscow State University, Leninskie Gory 1/3, 119991 Moscow, GSP-1, Russian Federation

^c International Tomography Center, Siberian Branch of the Russian Academy of Sciences, Institutskaya Str. 3a, 630090 Novosibirsk, Russian Federation

^d Kotel'nikov Institute of Radioengineering and Electronics, Russian Academy of Sciences, Mokhovaya Str. 11-7, 125009 Moscow, Russian Federation

ARTICLE INFO

Article history:

Received 27 June 2011

Received in revised form

19 September 2011

Accepted 24 September 2011

Available online 20 October 2011

Keywords:

Thulium pivalate

Coordination polymer

Synthesis

X-ray diffraction study

Magnetic and luminescence properties

Thermal behavior

ABSTRACT

The new 1D coordination polymer $\{\text{Tm}(\text{Piv})_3\}_n$ (**1**), where $\text{Piv} = \text{OOCBu}^{\text{t-}}$, was synthesized in high yield (> 95%) by the reaction of thulium acetate with pivalic acid in air at 100 °C. According to the X-ray diffraction data, the metal atoms in compound **1** are in an octahedral ligand environment unusual for lanthanides. The magnetic and luminescence properties of polymer **1**, its solid-phase thermal decomposition in air and under argon, and the thermal behavior in the temperature range of $-50 \dots +50$ °C were investigated. The vaporization process of complex **1** was studied by the Knudsen effusion method combined with mass-spectrometric analysis of the gas-phase composition in the temperature range of 570–680 K.

© 2011 Elsevier Inc. All rights reserved.

1. Introduction

Unusual magnetic, optical, and catalytic properties of organic-bridged lanthanide coordination polymers, including carboxylate bridged derivatives, have attracted considerable attention due to the fact that these compound hold promise in modern technologies as molecular-based materials combining various functional possibilities [1–14]. Among these compounds, polymeric carboxylates are of particular interest because, on the one hand, simple methods are available for their synthesis and, on the other hand, the molecular and supramolecular architectures can be varied in a wide range by changing the nature of the metal or the carboxylate anion or introducing additional donor ligands. It may be expected that the newly designed molecules will exhibit unusual anomalies in physical and chemical properties.

In complex carboxylates, lanthanide ions including thulium generally have large coordination numbers (8–12) and, as a rule, bind different numbers of neutral donor ligands, for example, water molecules or other solvents, depending on the steric capacity of the inner coordination sphere, which has a substantial

effect on the thermal stability of compounds associated with decomposition of organic compounds and, as a result, on the functional characteristics of the molecular-based material. Lanthanide carboxylate polymers, which do not contain additional inner-sphere ligands, are also known, but they were less well studied in the structural aspect (Cambridge Structural Database, version 5.32, updated November 2010 [15]), [16–19], which greatly complicates the comprehensive study of their physicochemical properties [4]. It should be noted that lanthanide carboxylates with the coordination number 6 are poorly known; only a few polymeric [20–25] and polynuclear compounds [26] were documented. However, of the 15 lanthanide elements Tm is the third smallest after Lu and Yb and so smaller coordination numbers would be expected for Tm^{3+} ion. Among carboxylate derivatives of thulium, several complexes [19,27–30] were structurally characterized. It was found that in mononuclear complex fragments [27–29] thulium(III) have coordination numbers 6, unlike that in polymeric systems [19,30] thulium as the other lanthanide ions demonstrated more saturated inner coordination sphere owing to diverse coordination modes presented by the carboxylate groups.

As for the optical properties of such molecular-based materials, it should be noted that attention has been focused on the optical properties of Eu^{3+} and Tb^{3+} ions due mainly to their

* Corresponding author. Fax: +7 495 952 1279.

E-mail address: fomina@igic.ras.ru (I. Fomina).

practical application as red and green luminescence emitters, respectively. Much less attention has been given to the Tm^{3+} ion exhibiting blue-color emission, which, in combination with Tb^{3+} (green) and Eu^{3+} (red) ions, may result in full-color emission phosphors [31,32]. Usually, Tm^{3+} complexes show only very weak $4f-4f$ luminescence as a consequence of a small energy gap between their emitting and lower energy levels; this increases the probability of non-radiative transitions through coupling with vibrational modes in the ligands [33]. The literature has mainly focused on the spectroscopic study of systems containing the Tm^{3+} ion formed by different inorganic matrices and there are some examples considered both the Tm^{3+} coordination polymers [34] and complexes.

The aim of the present study was to synthesize “ligand-free” polymeric thulium(III) pivalate. The pivalate anions containing the branched electron-donating *tert*-butyl substituent can partially shield the inner coordination sphere of lanthanide atoms from additional interactions, for example, with water or organic solvent molecules, which provides the basis for the design of formally coordinatively unsaturated polymeric carboxylate architectures. In addition, since lanthanide pivalates exhibit high volatility on heating *in vacuo* [35–37], thulium pivalates hold promise for the preparation of thin films by deposition onto various substrates. Hence, in addition to the magnetic and luminescence properties, in the present study we report on the results of the solid-phase thermal decomposition, the vaporization process, and the thermal behavior in the temperature range of $-50 \dots +50$ °C of polymeric thulium(III) pivalate.

2. Experimental

2.1. Synthesis

The synthesis was performed using the standard Schlenk techniques. Compound **1** was prepared with the use of HPiv (Acros Organics) and $\text{Tm}(\text{OOCCH}_3)_3 \cdot x\text{H}_2\text{O}$ (Alfa Aesar).

2.1.1. Synthesis $\{\text{Tm}(\text{Piv})_3\}_n$ (**1**)

Pivalic acid (7.83 mmol) was added to $\text{Tm}(\text{OOCCH}_3)_3 \cdot x\text{H}_2\text{O}$ (0.50 mmol). The reaction mixture was stirred in air at 100 °C until colorless crystals were formed. Then the reaction mixture was cooled to room temperature and kept for 24 h. The crystals were washed with cold hexane. The yield of compound **1** was 95%. Found (%): C, 38.16; H, 5.78. Calculated for $\text{C}_{15}\text{H}_{27}\text{O}_6\text{Tm}_1$ (%): C, 38.15; H, 5.76. IR (KBr), ν , cm^{-1} : 3079 w, 2955 s, 2924 s, 2865 m, 1592 s, 1574 s, 1527 s, 1513 s, 1484 s, 1456 m, 1428 s, 1376 m, 1360 s, 1305 w, 1260 w, 1230 s, 1139 w, 1102 w, 1030 w, 1016 w, 986 w, 937 w, 898 s, 864 m, 857 m, 810 m, 795 m, 735 m, 726 m, 640 m, 610 m, 588 m, 566 m, 536 m, 474 m, 451 w, 439 w, 420 w.

2.2. Methods

The H_2O content in $\text{Tm}(\text{OOCCH}_3)_3 \cdot x\text{H}_2\text{O}$ was determined by thermogravimetric analysis. The elemental analysis of compound **1** was carried out on an Euro Vector Element Analyser CHN elemental analyzer (Model EA 3000) and the diffuse reflectance IR spectrum was recorded on a NEXUS Infrared Fourier-transform spectrometer ($4000-400 \text{ cm}^{-1}$) in the Center of Collaborative Research of the N.S. Kurnakov Institute of General and Inorganic Chemistry of the Russian Academy of Sciences. The magnetic properties of compound **1** was measured on a MPMSXL SQUID magnetometer (Quantum Design) in the temperature range of 2–300 K in a magnetic field of up to 0.5 T. The paramagnetic components of the magnetic susceptibility χ were determined taking into account the diamagnetic contribution evaluated from

Pascal's constants. The temperature-dependent effective magnetic moment was calculated by the equation $\mu_{\text{eff}} = [(3k/N\beta^2) \cdot \chi T]^{1/2} \approx (8\chi T)^{1/2}$, where N is Avogadro's number, k is the Boltzmann constant, and β is the Bohr magneton. The luminescence and excitation spectra were measured at 300 and 77 K on a Fluorolog FL 3-22 Horiba–Jobin–Yvon spectrofluorometer, respectively. The photomultiplier response did not allow us to measure the emission spectrum beyond 850 nm.

2.3. X-ray data collection

The X-ray diffraction data for **1** were collected according to a standard procedure [38] on a Bruker APEX-II CCD diffractometer equipped with a CCD detector ($\text{Mo } K\alpha$, $\lambda = 0.71073$ Å). A semi-empirical absorption correction was applied (min/max transmission was 0.4870/0.8001) [39]. The structure was solved by direct methods and using Fourier techniques and was refined by the full-matrix least squares against F^2 with anisotropic thermal parameters for all non-hydrogen atoms. The hydrogen atoms of the carbon-containing ligands were positioned geometrically and refined using the riding model. In the crystal structure of **1**, there is one crystallographically independent pivalate group that lies on a twofold axis (the twofold axis passes through the C(1) and C(2) atoms of the pivalate ligand), resulting in the disorder of the *tert*-butyl group. The calculations were carried out with the use of the SHELX97 program package [40]. For **1**: $\text{C}_{15}\text{H}_{27}\text{O}_6\text{Tm}$, *fw* 472.30, $T = 150(2)$ K, trigonal crystal system, space group $P-3c1$, $a = 10.7469(7)$ Å, $b = 10.7469(7)$ Å, $c = 9.5447(7)$ Å, $\alpha = 90^\circ$, $\beta = 90^\circ$, $\gamma = 120^\circ$, $V = 954.68(11)$ Å³, $Z = 2$, $D_{\text{calc}} = 1.643$ mg cm^{-3} , $\mu = 4.668$ mm⁻¹, total number of reflections/unique reflections were 9269/796, $R_{\text{int}} = 0.0430$, $\theta_{\text{max}} = 28.27$, $S = 1.000$, R_1 ($I > 2\sigma(I)$) = 0.0552, wR_2 ($I > 2\sigma(I)$) = 0.1672, R_1 (all data) = 0.0671, wR_2 (all data) = 0.1778.

2.4. Mass spectrometry

The vaporization of complex **1** was studied by the Knudsen effusion method combined with mass-spectrometric analysis of the gas-phase composition in the temperature range of 570–680 K (297–407 °C) on a MC 1301 instrument. The experiments were carried out in a standard molybdenum cell with a vaporization surface-to-effusion orifice area ratio of ≈ 600 . The temperature was measured with a Pt–Pt(Rh) thermocouple with a constant accuracy of $\pm 1^\circ$. The mass spectrum of the gas phase over compound **1** is presented in Table 1.

2.5. Heat capacity

Experimental and calculation procedures on the determination of the isobaric heat capacity by differential scanning calorimetry (DSC) were carried out according to the ASTM E1269 – 95 standard test method. The experimental data were processed with the use of the NETZSCH Proteus Thermal Analysis software package described in [41].

Table 1

Mass spectrum of the gas phase over compound **1** ($T = 669$ K, $U_{\text{ioniz.}} = 60$ V).

Ion	$I_{\text{rel.}}$	Ion	$I_{\text{rel.}}$
TmO^+	6.7×10^{-3}	$[\text{Tm}_2(\text{Piv})_3\text{O}]^+$	0.029
$\text{Tm}(\text{Piv})^+$	0.035	$[\text{Tm}_2(\text{Piv})_3\text{COH}]^+$	0.26
$[\text{Tm}(\text{Piv})_2-3(\text{CH}_3)]^+$	0.02	$[\text{Tm}_2(\text{Piv})_4\text{O}]^+$	0.08
$\text{Tm}(\text{Piv})_2^+$	0.48	$[\text{Tm}_2(\text{Piv})_5-\text{CH}_3]^+$	0.058
$[\text{Tm}_2(\text{Piv})\text{COH}]^+$	0.11	$\text{Tm}_2(\text{Piv})_5^+$	1.0
$[\text{Tm}_2(\text{Piv})_2\text{O}]^+$	6.9×10^{-3}	$[\text{Tm}_2(\text{Piv})_5\text{O}_2\text{H}]^+$	2.9×10^{-3}
$[\text{Tm}_2(\text{Piv})_2\text{COH}]^+$	0.027	$[\text{Tm}_2(\text{Piv})_6-2(\text{CH}_3)]^+$	1.1×10^{-3}

The heat capacity was measured in special aluminum containers ($V=56\text{ mm}^3$, $d=6\text{ mm}$) equipped with a lid with a hole (the ratio of the surface area of the bottom of the cell to the surface area of the hole was about 36). The samples were weighted with an accuracy of $1 \times 10^{-2}\text{ mg}$. The average weight of the samples was ca. 10 mg. The measurements were carried out on a NETZSCH 204 F1 instrument in a dry argon stream (10 ml/min) at a heating rate of 10 K/min. The temperature calibration of the instrument was performed with the standard ISO/CD 11357-1 based on the phase transition points of reference compounds (C_6H_{12} , Hg, KNO_3 , In, Sn, Bi, CsCl; 99.99% purity). Synthetic sapphire ($m=12.69\text{ mg}$) was used as a standard material for the heat flow calibration.

For each sample, at least three series of measurements were carried out. The results of the measurements are given in Table 2.

The regular component of the heat capacity of complex **1** in the overall temperature range was approximated by the Berman–Brown polynomial equation: [42]

$$C_p(T) = k_0 + k_1 T^{-0.5} + k_2 T^{-2} + k_3 T^{-3}, \quad (1)$$

The validity of the model and the statistical significance of the coefficients of Eq. (1) were estimated by the Fisher exact test.

The absolute entropies of complex **1** were calculated from the limited region of the heat capacity curve by the extrapolation of the results of the DSC measurements of the heat capacity from the boiling point of liquid nitrogen to the zero temperature (0 K). This method gives the physically correct behavior of the temperature dependences of the heat capacity and provides the mathematically accurate standard entropies [41]. The regular component of the heat capacity of complex **1** was extracted and approximated to 0 K with the use of the following function

$$C_p(T) = \sum_i a_i C_{En} \left(\frac{\theta_i}{T} \right), \quad (2)$$

where $C_{En}(x) = 3Rx^2(\exp(x)/[\exp(x)-1]^2)$, $x = (\theta/T)$. The statistically best results were obtained for the polynomial (1) with two terms.

The standard entropy S_{298}° of complex **1** was estimated by the equation

$$S(T) = \sum_i a_i S_{En} \left(\frac{\theta_i}{T} \right), \quad (3)$$

where $S_{En}(x) = 3R[(x/(\exp(x)-1)) - \ln(1 - \exp(-x))]$, $x = (\theta/T)$.

Table 2
Temperature dependence of the heat capacity of compound **1**.

T (K)	C_p (J/mol K)	T (K)	C_p (J/mol K)	T (K)	C_p (J/mol K)
153	352.5	258	501.3	428	655.3
158	364.8	263	508.6	433	660.3
163	385	268	514.8	438	665.2
168	398	273	520.5	443	669.1
173	409.3	278	528.1	448	673.4
178	413.1	283	533.6	453	678
183	419.5	288	538.4	458	681.9
188	432.4	293	543.4	463	685.3
193	444.2	298	545.5	468	688.9
198	454	303	546.9	473	694.5
203	461.4	298	545.5	478	698.3
208	465.6	303	546.9	483	702.4
213	470.1	383	618.9	488	705.5
218	473.2	388	621.9	493	709.2
223	475.1	393	624.9	498	713.1
228	477	398	627.4	503	717.9
233	479.4	403	631.1	508	721.8
238	482.3	408	637.2	513	726
243	484.7	413	642.9	518	729.5
248	486.8	418	647.2	523	733.4
253	496.2	423	651.3	529	737.2

The estimation was performed taking into account the change in the entropy due to the transition associated with the anomaly in the curve C_p according to the equation $\Delta S_{T_{onset}}^- = (AREA/T_{onset})$, where AREA is the measured peak area in the experimental plot of the heat capacity versus the temperature.

2.6. Thermal decomposition

The thermal behavior of compound **1** was studied in an argon flow (20 ml/min) (Ar, > 99.998%; O_2 , 0.0002%; N_2 , 0.001%; water vapor, < 0.0003%; CH_4 , 0.0001%) and in an artificial air flow (20 ml/min) (O_2 , 20.8%; CH_4 , 0.0001%) by differential scanning calorimetry (DSC) and thermogravimetric analysis (TGA). The thermogravimetric analysis was performed on a NETZSCH TG 209 F1 instrument in alundum crucibles at a heating rate of 10 °C/min. The composition of the gas phase was studied by thermogravimetry-mass spectrometry on a QMS 403C Aolos mass-spectrometric unit. The ionizing electron energy was 70 eV; the largest determined mass number (the mass-to-charge (Z) ratio) was 300 amu. The weight of the samples used for TGA was 0.5–3 mg. The DSC studies were carried out on a NETZSCH DSC 204 F1 calorimeter in aluminum cells at a heating rate of 10 °C/min. The weight of the samples was 4–10 mg. The temperature calibration of the thermobalance was performed based on the phase transition points of the reference compounds. The calorimeter was calibrated against the temperature and the heat according to the standard ISO 11357-1. The samples used for the thermal analysis were weighed on a SARTORIUS RESEARCH R 160P analytical balance with an accuracy of $1 \times 10^{-2}\text{ mg}$. The thermal analysis data were processed with the use of the NETZSCH Proteus Thermal Analysis software package according to the standards ISO 11357-1, ISO 11357-2, and ISO 11358. The X-ray powder diffraction study of the decomposition products was carried out with a FR-552 monochromator chamber ($\text{CuK}\alpha_1$ radiation) using germanium as the internal standard (the X-ray diffraction patterns were measured on an IZA-2 comparator with an accuracy of $\pm 0.01\text{ mm}$) and with the use of the STOE Powder Diffraction System.

3. Results and discussion

3.1. Synthesis and X-ray diffraction study

Earlier [43,44], we have shown that the exchange reactions of aqueous lanthanide acetates with pivalic acid afford $\text{Ln}_2(\mu_2\text{-Piv})_4(\eta^1\text{-Piv})_2(\text{HPiv})_6 \cdot \text{HPiv}$ ($\text{Ln}=\text{La}, \text{Sm}, \text{Eu}, \text{Gd}, \text{and Er}$), in which metal atoms are easily coordinated by neutral organic N-donor ligands [44]. In the case of the complete removal of the coordinated neutral pivalic acid molecules from the starting carboxylates, resulting in the coordination- and electron-deficient molecules, polymer structures can be formed. Actually, the thermal decomposition of the dinuclear complexes at 180 °C afforded isostructural coordination polymers of the composition $\{\text{Ln}(\text{Piv})_3\}_n$ ($\text{Ln}=\text{Sm}, \text{Eu}, \text{Gd}, \text{and Er}$) characterized by X-ray powder diffraction [44].

As opposed to the above-mentioned thermal decomposition, polymeric thulium pivalate $\{\text{Tm}(\text{Piv})_3\}_n$ (**1**) is formed under relatively mild conditions, i.e., upon heating of $\text{Tm}(\text{OOCCH}_3)_3 \cdot x\text{H}_2\text{O}$ and an excess of pivalic acid in air at 100 °C, and does not contain coordinated neutral carboxylic acid. According to the single-crystal X-ray diffraction data, the crystal structure of **1** consists of 1D polymer chains, in which the adjacent thulium atoms are linked by three bidentate bridging carboxylate groups. Each thulium atom is in an almost ideal octahedral coordination formed by six oxygen atoms of six different pivalate anions

(Tm(1)–O(1), 2.176(8) Å) and has the low coordination number (6) unusual for lanthanide carboxylate complexes (Fig. 1).

Since the thulium atom lies on a special position (the crystallographic site $\bar{3}$), the chain consisting of thulium atoms is situated on a threefold inversion axis $\bar{3}$ (Fig. 1) (Tm...Tm, 4.772(1) Å; the TmTmTm angle, 180°). In the crystal structure, there is one crystallographically independent pivalate group, and its position on a twofold axis (the twofold axis passes through the C(1) and C(2) atoms of the pivalate ligand), resulting in the disorder of the *tert*-butyl substituent. Each of the three methyl groups has a symmetrical analog related by a twofold axis. In the crystal structure, the {Tm(Piv)₃}_n chains are separated from each other by the bulky *tert*-butyl groups of the pivalate ligands (Fig. 2). The distance between the chains running along the *a* (*b*) axis is 10.747 Å, which corresponds to the length of the crystallographic axis *a*.

Apparently, the pivalate anions containing branched electron-donating *tert*-butyl groups create steric hindrance to the saturation of the coordination sphere of thulium and can shield the thulium atom, thus hindering additional Tm–O interactions. The similar structure of the one-dimensional chain was found in the polymer {Sc(CH₃COO)₃}_n, in which the scandium atoms are linked by three bidentate bridging acetate anions [22].

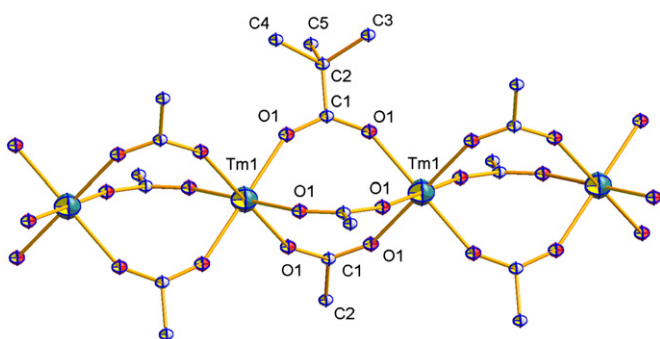


Fig. 1. Fragment of the polymer chain of compound 1.

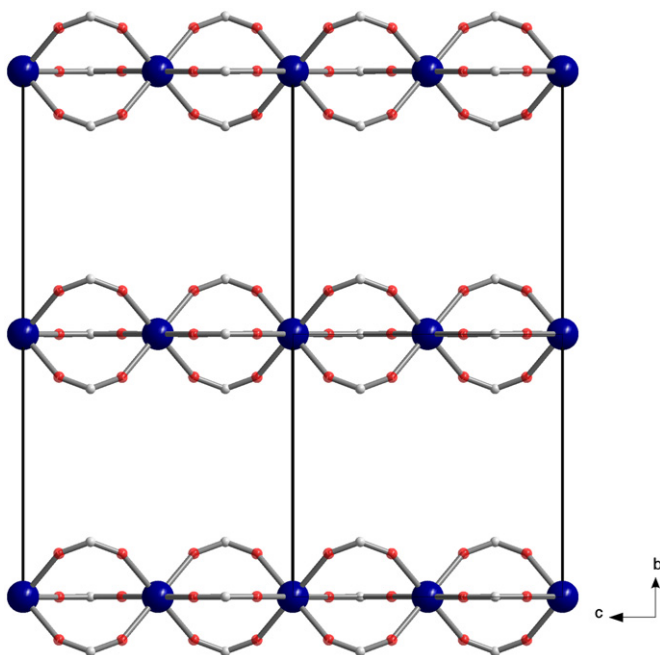


Fig. 2. Fragment of the crystal packing of compound 1.

3.2. Magnetic properties

The temperature dependence of the effective magnetic moment for {Tm(Piv)₃}_n is shown in Fig. 3. The magnetic moment μ_{eff} is

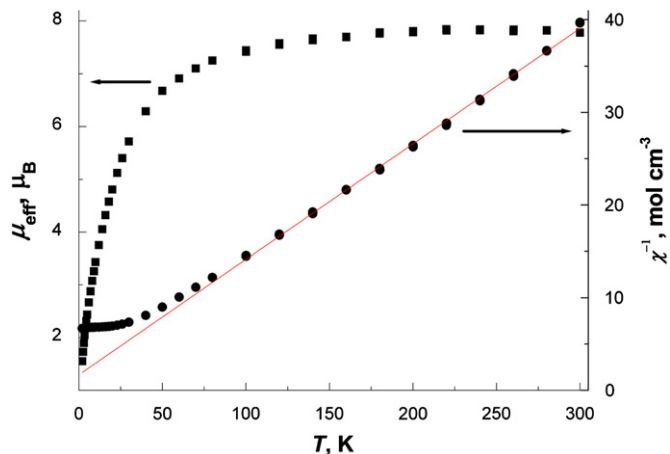


Fig. 3. Magnetic properties of compound 1 (the temperature dependence of the magnetic moment (■); the curve $1/\chi$ (●) and the calculated data represented by a line).

7.80 μ_{B} at 300 K and agrees well with the typical value for Tm(III) derivatives 7.57 μ_{B} ($\mu_{\text{eff}} = g_J [J(J+1)]^{1/2}$, ground state $^3\text{H}_6$, $g_J = 7/6$). The μ_{eff} value remains almost unchanged with a decrease in the temperature to 120 K and then gradually decreases to 1.55 μ_{B} at 2 K. The temperature dependence of the inverse magnetic susceptibility obeys the Curie–Weiss law with the parameters $C = 8.03 \text{ cm}^3 \text{ K/mol}$ and $\theta = -13 \text{ K}$ in the temperature range of 100–300 K.

3.3. Luminescence properties

The luminescence spectrum of thulium pivalate 1 recorded at 77 K ($\lambda_{\text{exc}} = 280 \text{ nm}$) is shown in Fig. 4. Based on the existing literature [45–47] the emission bands observed at 26600 cm^{-1} /375 nm, 25315 cm^{-1} /395 nm, 23955 cm^{-1} /420 nm, 22890 cm^{-1} /440 nm, and 21430 cm^{-1} /465 nm have been tentatively assigned to the $^1\text{D}_2 \rightarrow ^3\text{H}_6$, $^1\text{I}_6 \rightarrow ^3\text{H}_5$, $^1\text{D}_2 \rightarrow ^3\text{H}_4$, and $^1\text{D}_2 \rightarrow ^3\text{H}_5$ transitions of Tm^{3+} ion, respectively. The well-known $^1\text{G}_4 \rightarrow ^3\text{H}_6$ transition is not observed in this spectrum (its energy is typically $\sim 480 \text{ nm}$) while the several bands corresponded to the transitions from the $^1\text{D}_2$ level are

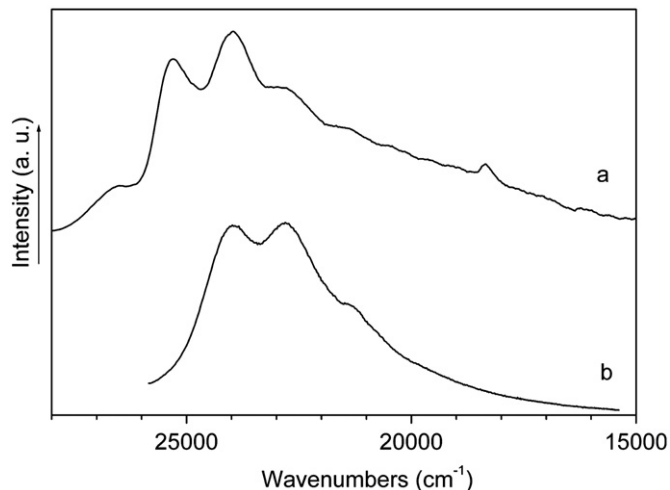


Fig. 4. Luminescence spectra of compound 1 at 77 (a) and 300 (b) K.

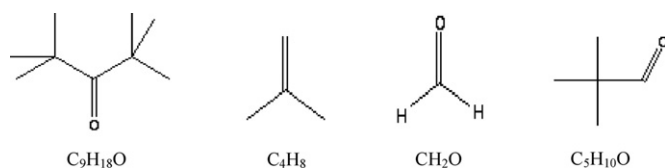
presented. Therefore the assignment performed is also in line with the fact that the Tm^{3+} ($4f^{12}$) ion is one of the most interesting Ln^{3+} ions in terms of the fluorescence properties because its emitting $^1\text{D}_2$ level exhibits high quantum efficiency [48]. Similar transitions of the Tm^{3+} ion are observed in the luminescence spectrum recorded at room temperature (Fig. 4b). Hence compound **1** exhibits blue-color emission, indicating that this coordination polymer can be used as an efficient light conversion molecular device (LCMD).

3.4. Thermal decomposition, mass spectrometry, and heat capacity

High functional characteristics are among the requirements placed on potential materials. However, investigations of chemical and thermal stability of compounds, as well as their thermal behavior, under operating conditions are also of considerable importance. When deciding about the use of substances in technologies, which involve vaporization or decomposition, it is important to know the thermal behavior of the complexes during heating both under normal pressure and *in vacuo*.

The investigation of the solid-phase thermal decomposition showed that compound **1** is stable up to 410 °C and 435 °C in air and under an inert atmosphere, respectively; at higher temperatures, the thermal decomposition occurs (Fig. 5). The completion of the decomposition under an inert atmosphere and in air was observed at 545 and 470 °C, respectively. In air, the redox decomposition accompanied by the exothermic effect $Q = 2050 \pm 100$ kJ/mol (of the monomer unit) occurs, whereas the formation of the solid decomposition product and the removal of volatile products under argon are endothermic with $Q = 326.5 \pm 30$ kJ/mol (of the monomer unit). The weights of the solid residue are $38.7 \pm 1.0\%$ (in air) and $40.5 \pm 1.0\%$ (under argon) and are almost equal to the value calculated on the assumption that the thermal decomposition affords thulium(III) oxide (40.8%). The phase composition of the solid product was confirmed by the X-ray powder diffraction data. It should be noted that polymer **1**, like the coordination polymers $\{\text{Ln}(\text{Piv})_3\}_n$ ($\text{Ln} = \text{Sm}, \text{Eu}, \text{Gd}, \text{and Er}$), is stable to atmospheric moisture over a long period of time (for more than a year).

Under an inert atmosphere, the gas-phase mass spectrum obtained in the temperature range of 435–545 °C showed the following ions: C^+ (12), CO^+ (28), CO_2^+ (44), CH_2^+ (14), CH_3^+ (15), C_2H_3^+ (27), C_2H_4^+ (28), C_2H_5^+ (29), CHO^+ (29), C_3H_5^+ (41), C_3H_6^+ (42), C_3H_7^+ (43), C_4H_8^+ (56), C_4H_9^+ (57), $\text{C}_5\text{H}_9\text{O}^+$ (85). According to the results of the study [49], the possible thermal decomposition products of **1** in the gas phase are



Earlier [49], we have calculated the composition of the multi-component heterogeneous system from the evaluation thermodynamic data for *tris*-pivalates $\text{Ln}_2(\text{Piv})_6$ ($\text{Ln} = \text{La}, \text{Sm}, \text{and Eu}$). Based on these data, the possible overall scheme of the thermolysis of these compounds has been suggested. Taking into account the results of the study [49] and the analysis of the above-mentioned mass spectrum and the mass spectra of possible volatile products [50], the probable scheme of the thermolysis of complex **1** under an inert atmosphere can be written as:



The investigation of the vaporization of complex **1** provided convincing evidence that the dinuclear molecules $\text{Tm}_2(\text{Piv})_6$ are

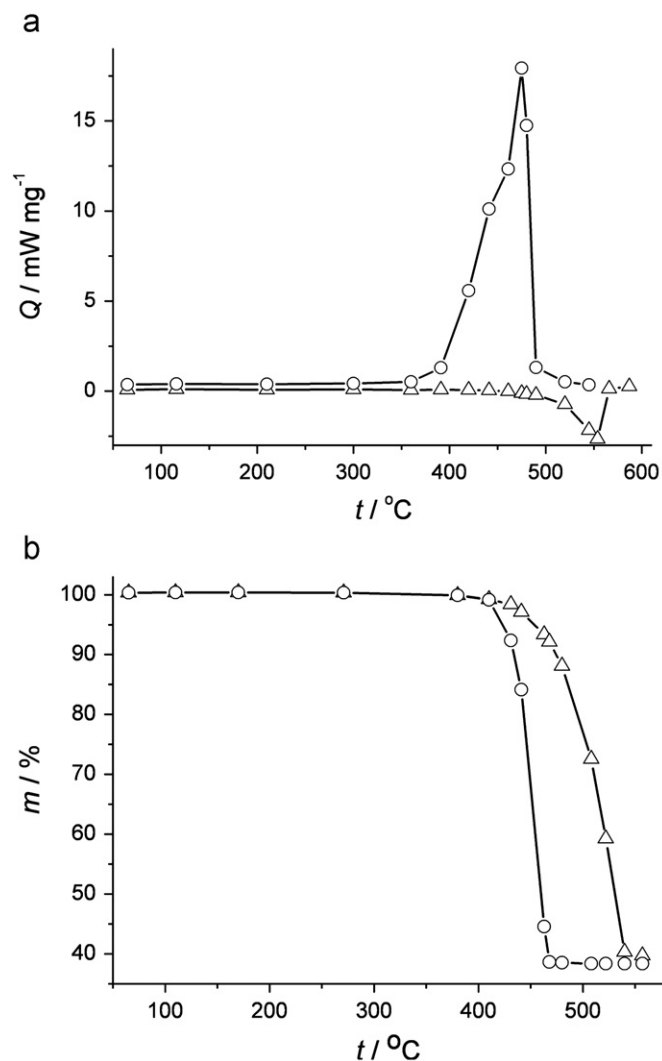
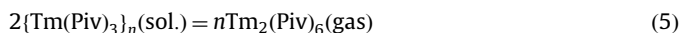


Fig. 5. Plots of the heat flux (a) and the weight loss (b) versus the temperature during heating of compound **1** (○, in air; △, under an inert atmosphere).

present in the gas phase over the complex $\{\text{Tm}(\text{Piv})_3\}_n$ (Table 1). However, the mass spectrum shows the second strongest $I_{\text{Tm}(\text{Piv})_2^+}$ of the ion current, which can be assigned to both the mononuclear and dinuclear molecules. To determine the vapor composition and the character of vaporization of complex **1**, we performed experiments on the complete isothermal sublimation of samples of a known weight from the standard and double effusion cells. The fact that the intensities of all ion currents remained constant until the samples were completely burned out and the absence of a non-volatile residue after vaporization of the sample from the standard cell are unambiguously indicative of the congruent character of sublimation of compound **1**, *i.e.*, the overall compositions of the gas and condensed phases are equal in the course of sublimation. The vaporization of the weighed samples (q_I, q_{II}) from the double effusion cell provides information on the qualitative composition of the saturated vapor over thulium pivalate. The initially constant ion current intensities correspond to the mass spectrum of the saturated vapor (Table 1) upon sublimation of the weighed sample q_I from the upper part of the Knudsen cell. A sharp decrease in the ion current intensities is attributed to the burning out of the sample. The intensities that again became constant correspond to the mass spectrum of the unsaturated vapor upon sublimation of the sample q_{II} of thulium

pivalate from the lower part of the cell. The qualitative gas-phase composition was estimated from the analysis of the changes in the ion current intensities. In the case of the effusion hole area ratio of the upper to lower parts of the cell equal to *ca.* 2, the intensities of the ions containing one and two thulium atoms decrease in parallel with each other by a factor of 20. This change in the ion currents indicates that only the dinuclear molecule $\text{Tm}_2(\text{Piv})_6$ is their molecular precursor. Consequently, the vaporization of thulium pivalate can be described by the reaction:



The pressure of the dinuclear molecules was calculated from the experiments on complete isothermal sublimation by the Hertz–Knudsen equation. At $T=679\text{ K}$, $P_{\text{Tm}_2(\text{Piv})_6}=6.4 \times 10^{-1}\text{ Pa}$. The enthalpy of the reaction (5) was determined from the second law of thermodynamics based on the temperature dependences of the ion current intensities $I_{\text{Tm}(\text{Piv})^+}$, $I_{\text{Tm}(\text{Piv})_2^+}$, $I_{[\text{Tm}_2(\text{Piv})\text{COH}]^+}$, $I_{[\text{Tm}_2(\text{Piv})_3\text{COH}]^+}$, and $I_{\text{Tm}_2(\text{Piv})_5^+}$ in the temperature range of 587–670 K. The standard enthalpy of sublimation was calculated by the Clausius–Clapeyron equation by the least squares. The enthalpies of sublimations evaluated for five different ions from seventeen independent measurements are in good agreement, within experimental error, with each other. The average value

Table 3

Coefficients of the polynomial (1).

K_0	$-k_1 \times 10^{-3}$	$k_2 \times 10^{-6}$	$-k_3 \times 10^{-8}$
1920	30.66	49.8	43.8

$\Delta_S H^0[\{\text{Tm}(\text{Piv})_3\}_n, \text{sol.}, T] = 228.8 \pm 3.6\text{ kJ/mol}$. The error in the determination is the rms error of the mean of a series of measurements. This result can be considered as a direct evidence for the validity of the interpretation of the mass spectrum and, consequently, the correctness of the calculation of the gas-phase composition. If it were not so, the enthalpies determined based on different ions would be different.

Fig. 6 shows the temperature dependences of the heat flux during heating and cooling in the temperature range from -50 to $200\text{ }^\circ\text{C}$ (6a), as well as the experimental values and the temperature dependence of the regular component of the heat capacity calculated by Eq. (1) with the coefficients presented in Table 3 (the coefficient of determination was 0.9987; the prediction error for the heat capacity was 3.7 J/mol K). The curves of the heat capacity for thulium bis-pivalate exhibit a reproducible anomaly (Fig. 6). It should be noted that the parameters of the peak do not depend on the thermal history of the sample (the final temperature and the rate of cooling), the hysteresis with respect to the temperature of the extremum is absent, the peak has the characteristic λ shape, and the temperature of the maximum does not depend on the experimental conditions (including, the weight of the sample) and is $66.9 \pm 0.3\text{ }^\circ\text{C}$. Hence, this anomaly can be assigned with a high probability to the second-order phase transition. The evaluated value S_{298}^0 for complex **1** is $(460 \pm 11)\text{ J/mol K}$.

4. Conclusions

In summary, we synthesized the Tm^{3+} coordination polymer $\{\text{Tm}(\text{Piv})_3\}_n$ stable to atmospheric moisture by an easy one-step method (by the exchange reaction of $\text{Tm}(\text{OOCCH}_3)_3 \cdot x\text{H}_2\text{O}$ with pivalic acid). It was shown that the metal atoms in this material have the coordination number 6, which is rather rare for large lanthanide ions. Polymer **1** exhibits blue-color emission at room temperature (centered at 450 nm), shows high thermal stability, and is characterized by the absence of phase transitions in the temperature range of $-50 \dots +50\text{ }^\circ\text{C}$ and volatility. These data provide evidence that compound **1** can be used as an efficient blue component in full-color systems.

Acknowledgments

This study was financially supported by the Russian Foundation for Basic Research (Project nos. 10-03-00515), the Council on Grants of the President of the Russian Federation (Grants NSh-3672.2010.3, NSh-8503.2010.3), the Ministry of Education and Science of the Russian Federation (SC-14.740.11.0363), the Target Programs for Basic Research of the Presidium of the Russian Academy of Sciences, and the Division of Chemistry and Materials Science of the Russian Academy of Sciences. The work was partially performed at the User Facilities Center of the M.V. Lomonosov Moscow State University.

Appendix A. Supplementary materials

Supplementary data associated with this article can be found in the online version at doi:10.1016/j.jssc.2011.09.033.

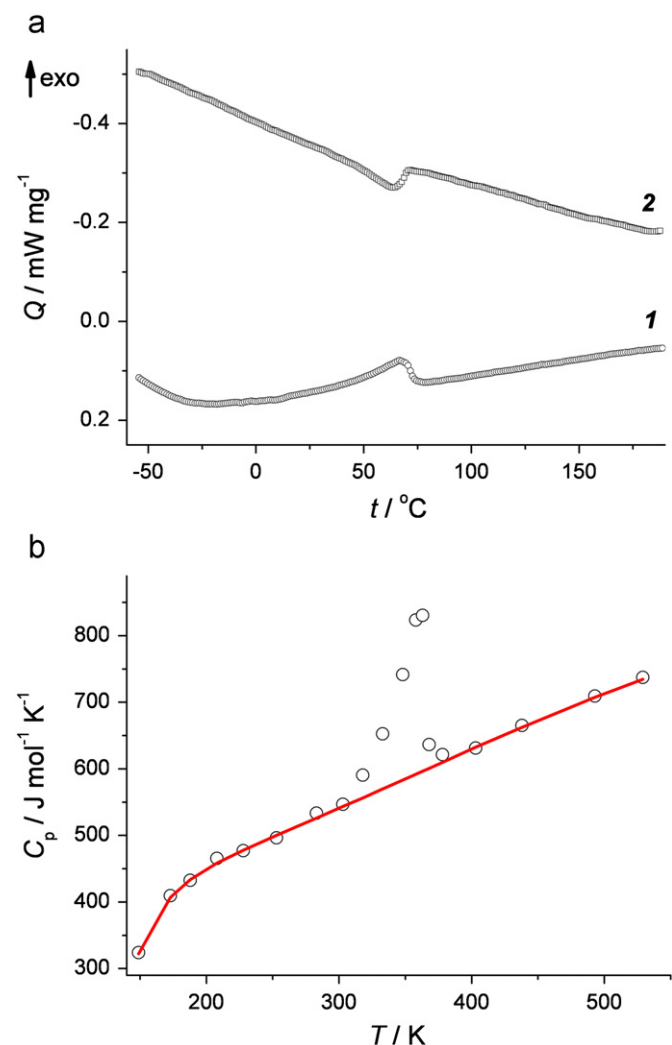


Fig. 6. (a) Plots of the heat flux versus the temperature: 1, heating; 2, cooling; (b) the temperature dependence of the molar heat capacity: \circ , experimental data, —, calculations.

References

- [1] S. Kitagawa, R. Kitaura, S.-I. Noro, *Angew. Chem. Int. Ed.* 43 (2004) 2334–2375.
- [2] G. Ferey, *Chem. Soc. Rev.* 37 (2008) 191–214.
- [3] L. Ma, C. Abney, W. Lin, *Chem. Soc. Rev.* 38 (2009) 1248–1256.
- [4] O. Guillou, C. Daiguebonne, Lanthanide-containing Coordination Polymers, in: K.A. Gschneidner Jr., J.-C.G. Bünzli, V.K. Pecharsky (Eds.), *Handbook on the Physics and Chemistry of Rare Earths* 34, Elsevier, Amsterdam, 2005 Chapter 221.
- [5] D.L. Long, A.J. Blake, N.R. Champness, C. Wilson, M. Schroder, *Chem. Eur. J.* 8 (2002) 2026–2033.
- [6] R. Gheorghie, P. Cucos, M. Andruh, J.P. Costes, B. Donnadieu, S. Shova, *Chem. Eur. J.* 12 (2006) 187–203.
- [7] M.D. Allendorf, C.A. Bauer, R.K. Bhakta, R.J.T. Houk, *Chem. Soc. Rev.* 38 (2009) 1330–1352.
- [8] K. Binnemans, *Chem. Rev.* 109 (2009) 4283–4374.
- [9] J. Kido, Y. Okamoto, *Chem. Rev.* 102 (2002) 2357–2368.
- [10] C. Benelli, D. Gatteschi, *Chem. Rev.* 102 (2002) 2369–2388.
- [11] G. Adachi, N. Imanaka, S. Tamura, *Chem. Rev.* 102 (2002) 2405–2430.
- [12] C.J. Weiss, T.J. Marks, *Dalton Trans.* 39 (2010) 6576–6588.
- [13] S. Capecchi, O. Renault, D.G. Moon, M. Halim, M. Etchella, P.J. Dobson, O.V. Salata, V. Christou, *Adv. Mater.* 12 (2000) 1591–1594.
- [14] L. Pan, K.M. Adams, H.E. Hernandez, X. Wang, C. Zheng, Y. Hattori, K. Kaneko, *J. Am. Chem. Soc.* 125 (2003) 3062–3067.
- [15] F.H. Allen, *Acta Crystallogr., Sect. B: Struct. Sci.* B58 (2002) 380–388.
- [16] S.G. Torres, G. Meyer, *Z. Anorg. Allg. Chem.* 634 (2008) 231–233.
- [17] A. Lossin, G. Meyer, *Z. Anorg. Allg. Chem.* 620 (1994) 438–443.
- [18] S.G. Torres, I. Pantenburg, G. Meyer, *Z. Anorg. Allg. Chem.* 632 (2006) 1989–1994.
- [19] A. Lossin, G. Meyer, *Z. Anorg. Allg. Chem.* 619 (1993) 1609–1615.
- [20] D.T. de Lill, C.L. Cahill, *Chem. Commun.* 47 (2006) 4946–4948.
- [21] X. Li, Z.-Y. Zhang, D.-Y. Wang, Y.-Q. Zou, *Z. Kristallogr.—New Cryst. Struct.* 220 (2005) 36–38.
- [22] M.K. Guseinova, A.S. Antsishkina, M.A. Poray-Koshits, *J. Struct. Chem. (USSR) (Engl. Transl.)* 9 (1968) 1040–1045.
- [23] N.G. Furmanova, Z.P. Razmanova, L.V. Soboleva, I.A. Maslyanitsin, H. Siebert, V.D. Shigorin, G.P. Shipulo, *Sov. Phys.—Crystallogr. (Engl. Transl.)* 29 (1984) 476–479.
- [24] P. Kistaiah, K.S. Murthy, L. Iyengar, K.V.K. Rao, *J. Mater. Sci.* 16 (1981) 2321–2323.
- [25] M.A. Poray-Koshits, A.S. Antsishkina, G.G. Sadikov, G.A. Kukina, *Sov. Phys.—Crystallogr. (Engl. Transl.)* 16 (1971) 1195–1202.
- [26] X.-Y. Chen, Y. Bretonniere, J. Pecaut, D. Imbert, J.-C. Bunzli, M. Mazzanti, *Inorg. Chem.* 46 (2007) 625–637.
- [27] M.A. Nabar, S.D. Barve, *J. Appl. Crystallogr.* 17 (1984) 39.
- [28] M.A. Nabar, S.D. Barve, *J. Appl. Crystallogr.* 16 (1983) 576.
- [29] B. Klimek, A.E. Koziol, K. Stepniak, *Z. Kristallogr.* 174 (1986) 305–307.
- [30] G.-M. Wang, C.-S. Duan, H.-L. Liu, H. Li, *Acta Crystallogr. E64* (2008) m468–m469.
- [31] A.J. Steckl, J. Heikenfeld, D.S. Lee, M. Garter, *Mater. Sci. Eng. B* 81 (2001) 97–101.
- [32] J. Feng, H.J. Zhanga, S.Y. Song, Z.F. Li, L.N. Sun, Y. Xing, X.M. Guo, *J. Lumin.* 128 (2008) 1957–1964.
- [33] H.F. Brito, O.L. Malta, M.C.F.C. Felinto, E.E.S. Teotonio, The chemistry of metal enolates, in: J. Zabicky (Ed.), *Luminescence Phenomena Involving Metal Enolates*, 1, John Wiley & Sons Ltd., England, 2009, pp. 131–184 Chapter 3.
- [34] J. Qin, D. Du, L. Chen, X. Sun, Y. Lan, Z. Su, *J. Solid State Chem.* 184 (2011) 373–378.
- [35] N.P. Kuz'mina, L.I. Martynenko, T.A. Zoan, Ch.T. Nguet, S.I. Troyanov, A.N. Rykov, Yu.M. Korenev, *Russ. J. Inorg. Chem.* 39 (1994) 512–520.
- [36] I.P. Malkerova, A.S. Alikhanyan, I.G. Fomina, Zh.V. Dobrokhotova, *Russ. J. Inorg. Chem.* 55 (2010) 53–57.
- [37] A.L. Emelina, Zh.V. Dobrokhotova, A.A. Sinelshchikova, Yu.A. Velikodnyi, I.G. Fomina, P.S. Koroteev, V.M. Novotortsev, I.L. Eremenko, *Russ. J. Inorg. Chem.* 55 (2010) 1754–1761.
- [38] SMART (Control) and SAINT (Integration) Software, Version 5.0, Bruker AXS Inc., Madison, WI, 1997.
- [39] G.M. Sheldrick, SADABS, Program for Scanning and Correction of Area Detector Data, Göttingen University, Göttingen, Germany, 2004.
- [40] G.M. Sheldrick, SHELX-97: Program for the Solution of Crystal Structures, Göttingen, Germany, 1997.
- [41] M.A. Bykov, A.L. Emelina, E.V. Orlova, M.A. Kiskin, G.G. Aleksandrov, A.S. Bogomyakov, Zh.V. Dobrokhotova, V.M. Novotortsev, I.L. Eremenko, *Russ. J. Inorg. Chem.* 54 (2009) 548–557.
- [42] R.G. Berman, T.H. Brown, *Contrib. Mineral Petrol.* 89 (1985) 168–183.
- [43] I.G. Fomina, M.A. Kiskin, A.G. Martynov, G.G. Aleksandrov, Zh.V. Dobrokhotova, Yu.G. Gorbunova, Yu.G. Shvedenkov, A.Yu. Tsivadze, V.M. Novotortsev, I.L. Eremenko, *Russ. J. Inorg. Chem.* 49 (2004) 1349–1359.
- [44] Zh.V. Dobrokhotova, I.G. Fomina, G.G. Aleksandrov, Yu.A. Velikodnyi, V.N. Ikorskii, A.S. Bogomyakov, L.N. Puntus, V.M. Novotortsev, I.L. Eremenko, *Russ. J. Inorg. Chem.* 54 (2009) 668–685.
- [45] G.H. Dieke, *Spectra and Energy Levels of Rare Earth Ions in Crystals*, New York, Wiley, 1968.
- [46] W.T. Carnal, P.R. Fields, K. Rajnak, *J. Chem. Phys.* 49 (1968) 4424–4442.
- [47] U. Hommerich, E.E. Nyein, D.S. Lee, A.J. Steckl, J.M. Zavada, *Appl. Phys. Lett.* 83 (2003) 4556–4558.
- [48] Z. Mazurak, M. Czaja, R. Lisiecki, J. Gabrys-Pisarska, *Opt. Mater.* 33 (2011) 506–510.
- [49] Zh.V. Dobrokhotova, I.G. Fomina, M.A. Kiskin, M.A. Bykov, G.V. Belov, V.M. Novotortsev, *Russ. J. Phys. Chem.* 80 (2006) 323–329.
- [50] <<http://webbook.nist.gov>>.